The fabrication and characterization of granular aluminium/ palladium bilayer microbolometers

T E Wilson

Department of Physics, Marshall University, One John Marshall Drive, Huntington, WV 25755-2570 USA

wilsont@marshall.edu

Abstract. Superconducting granular aluminium / palladium bilayer microbolometers can be easily fabricated using an all lift-off process with image-reversal lithography. The palladium capping layer allows for convenient and reproducible Ohmic contacts to be made to the device. We report their fabrication, resistance-temperature calibration, responsivity and response time. Finally, a deconvolution algorithm is used to improve the time resolution to approximately 1 ns while obtaining the incident photon and phonon fluxes in both direct photoexcitation and phonon heat pulse experiments. PAC codes: 07.57.Kp, 42.82.Cr, 63.20.-e, 95.55.Rg, 74.81.Bd, 74.45.+C

Keywords: superconducting transition temperature, critical temperature, phonons, thin film bolometers, transition edge sensors.

1. Introduction

Much of the recent work in bolometry has been associated with the detection of particles and photons [1,2]. In these experiments, the bolometers act as sensitive microcalorimeters in a constant bias voltage mode. In such experiments the energy resolution is optimized. On the other hand, in studies of phonon transport in solids, time resolution requirements of less than 1 μs dictates that the bolometer be operated in a constant bias current mode [3] instead. Granular aluminium (GA) bolometers are often employed for this application. For example, Rani *et al* [4] used a GA bolometer of 100 by 100 μm area and a thickness of 20 nm to study ion bombarded sapphire surfaces in heat pulse experiments. The thermal response time of this bolometer was $\tau = 20$ ns. A deconvolution algorithm was developed to improve the time resolution to approximately 10 ns [5]. A GA microbolometer of dimension 6 by 30 μm area was used to study the quasidiffusive transport of optically generated acoustic phonons in Si [6]. The response time was 85 ns but degraded to 110 ns because of thermal cycling. A GA bolometer for the study of IR multiple photon resonances of polyatomic molecules was operated with a time constant of 60 ns [7].

One of the main shortcomings of GA bolometers is their short lifetime. It has been reported that the films have little mechanical strength, oxidize in air, and exhibit a tendency to suffer damage during cycling between room temperature and their operating temperature [8], and are difficult to make Ohmic contacts [9]. Although GA bolometers prepared in an oxygen atmosphere have been used for many years [10] as sensitive detectors of acoustic phonons, there does not seem to be in the literature a

detailed description for producing micrometer-sized GA bolometers with reliable Ohmic contacts. In this note, we provide a convenient recipe for fabricating reliable GA microbolometers with 1-10 nanosecond response time using photolithography and dc-magnetron sputtering, and our recipe requires no chemical or plasma etching. Our particular approach also solves the traditional problem for GA of unreliable (i.e., non-Ohmic) electrical contacts and degradation by oxidation by using a palladium capping layer on the GA film prior to exposure to air. Furthermore, our bolometers have undergone many (>20) thermal cycles during the course of a year with no degradation.

We report the typical transition temperature and width of the bilayer SC transition, the bolometer responsivity and response time, and perform a deconvolution of the raw bolometer signal to obtain both the incident flux of photons in a direct photoexcitation experiment, and the incident phonon flux in a heat pulse experiment.

2. Preparation of bilayer thin film bolometers

The SC films reported here have been patterned on polished 0.50 mm thick [100] float zone silicon die of dimension 12 mm x 16 mm. The resulting GA bolometers are each of nominal thickness 100 nm and with an active region consisting of a 10 micron x 20 micron GA / palladium bilayer that links two larger 1 mm x 2 mm chromium/gold contact pads (nominal thickness 140 nm).

We fabricate the bolometers using an all lift-off process with image-reversal lithography employing *AZ 5214E* photoresist and *AZ Developer*, as partially described in the literature [11]. In the image reversal process, the photoresist acts in the negative mode in that any area of the photoresist which is exposed through the mask remains after development. We have found that the image-reversal process, with backward-sloping sidewalls of the patterned photoresist, results in a significantly easier, faster, and higher quality liftoff in acetone of the undesired portion of the deposited metallic film. Prior to the first patterning only, the sample surfaces are chemically cleaned by successive 5 minute dips in (1) 10% hydrofluoric acid and (2) piranha [12] solutions. The die is then carefully centered on a small vacuum chuck of a *Headway PWM32* [13] and the photoresist is spun to a nominal thickness of 1.4 μm according to the recipe listed in Table 1. The hexamethyldisilizane (HMDS) adhesion promoter and the photoresist are manually dispensed with *Whatman Autovial* 0.2μm PTFE membrane filter devices [14].

The lithography procedure is outlined in Table 2. We expose the silicon die on a *Karl Suss MJB3* mask aligner through a chromium soda-lime photomask, supplied by *Adtek Photomasks, Inc.*, and designed by the author with *L-Edit* software [15]. Each 12 mm x 16 mm die (diced later into four 5 mm x 7 mm samples) is patterned with a 2 x 2 array of bolometers. It is imperative to use *AZ Developer* for GA since, unlike most positive photoresist developers, it does not etch aluminum.

Table 1. *AZ 5214 E* photoresist spin recipe.

Speed (rpm)	Ramp (rpm/s)	Duration (s)	Operation
3000	1500	30	Successive acetone, methanol, and isopropanol rinses
0	N/A	15	HMDS dispense
3000	1500	30	HMDS spin
0	N/A	15	Photoresist dispense
4000	300	45	Spin
10000	5000	3	Edge bead reduction

Table 2. *AZ 5214 E* Image-reversal photolithography recipe.

Spin *AZ5214 E* as per Table 1 recipe.
Hotplate softbake at 90 C for 60 s
Expose 16.0 mW/cm^2 405 nm CI2 for 9.4 s
Hotplate postbake at 115 C for 40 s
Flood expose 80 s
Develop in *AZ Developer* 1:1 at 23 C for 135 s
Rinse in deionized water, blow dry nitrogen

We use a *Denton Discovery 18* load-lock dual-target dc-magnetron sputter deposition system [16] retrofitted with an oxygen lecture bottle and a precision needle valve [17] arrangement. All metal films are sputtered at a dc-magnetron power of 400 W in an 8.5 mTorr argon plasma with an argon flow rate of 28 sccm through the chamber. For each metal, we also use a 2 minute burn-in period (shutter closed) prior to sputtering. For the GA deposition, two Si die are positioned side by side on the platen, the chamber is evacuated to a base pressure of 1 μTorr, oxygen is introduced and carefully adjusted to a pressure of 170 μTorr, then argon is introduced and the plasma struck; Al is then sputtered from the first target for 80 seconds (resulting in a nominal thickness of 100-nm). To prevent oxidation of the 100-nm thick GA surface during subsequent processing, a much thinner (5 nm) palladium film is sputtered (2-3 s) from a second target prior to breaking vacuum. The desired metallic pattern (1 mm long and 10 μm wide) is easily obtained by "lifting off" the undesired portion in a brief (30 s) acetone soak with ultrasonic agitation. The palladium capping layer consistently results in reliable electrical connection (no insulating barrier) to the overlying chromium/gold contacts fabricated later – a new finding. Generally, test runs are first made on clean glass cover slips in order to verify that the resulting room temperature resistivity (measured with a portable four-point probe) of the sputtered Ga / Pd bilayer is in the desired range (below). (Although the width of the active region of our bolometers is 10 μm, we have also patterned niobium grating-couplers with a line/space ratio of 3 μm/7 μm using the same lithography recipe.)

A subsequent patterning of the chromium/gold (1 mm x 2 mm) contact pads, spaced 20-μm apart and with the midpoint of the opening between the two pads centered on top of the 1 mm long GA/Pd bilayer, then completes the GA/Pd bolometer fabrication. The contact pads consist of a sputtered chromium adhesion layer (30 s results in a 20 nm nominal thickness), followed by a sputtered gold layer (45 s yields a 120 nm nominal thickness) using a second target, prior to breaking vacuum. Figure 1 shows the bolometer.

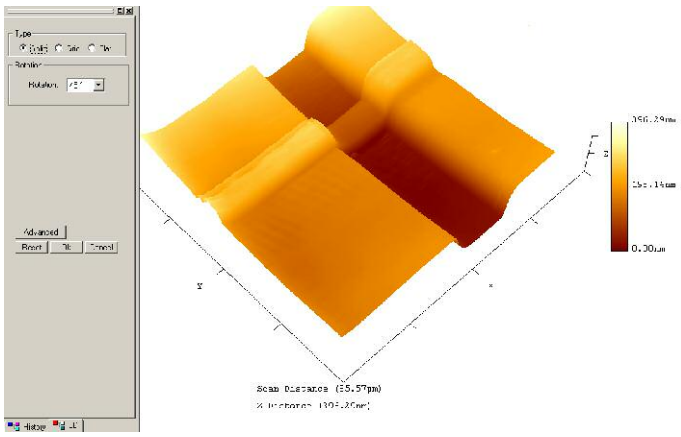

Figure 1 An atomic force microscope image of the microbolometer. The active region consists of a 10 μm x 20 μm GA / palladium bilayer of thickness 100 nm that lies beneath two larger 1 mm x 2 mm chromium/gold contact pads (thickness 140 nm)

3. Results

The resistivity versus (low) temperature characteristics of the GA / palladium bilayer deposited upon a glass slide have been obtained using a homemade four-point probe apparatus with a typical result is shown in Figure 2. Under the conditions noted above, the sputtered GA / palladium bilayer possesses a room temperature resistivity in the range of 25 to 35 μOhm-cm and a corresponding superconducting (SC) transition temperature near 1.8 K, in agreement with previous investigations of the superconductivity of GA alone [18]. The Pd capping layer is apparently sufficiently thin that there is no substantial suppression of the SC transition of the underlying GA layer due to the proximity effect [19]. For the sample displayed, the width (10-90%) of the SC transition is approximately 40 mK and

the midpoint of the transition occurs at 1.76 K. The sensitivity of these bolometers, $(dR/dT)/R_Q$ (where R is resistance, T is temperature and R_Q is the resistance mid point of the transition) varies somewhat bias current but is approximately 30 K^{-1}. Although the variation in the room temperature resistances of a 2 x 2 bolometer array patterned on a given die is generally within 10% (R_b~10 Ω), the die-to-die variation of the bolometer resistances is larger (~30%) as a result of the variation in the resistivity from different sputtering runs. No studies were done using a matrix of different Pd layer thicknesses to investigate how to fabricate a bolometer to operate at a particular temperature.

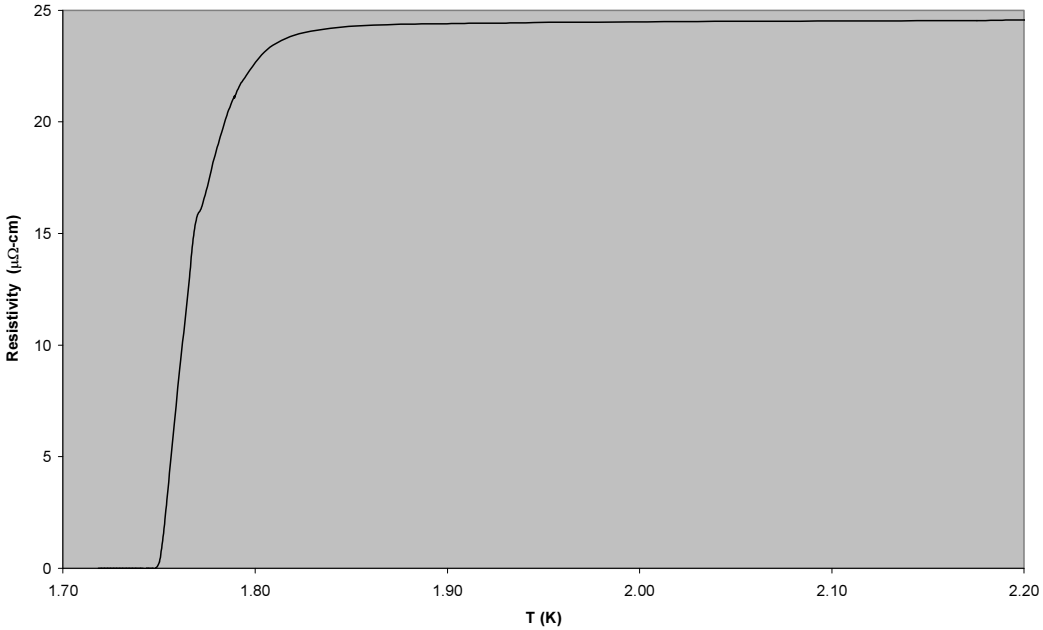

Figure 2. Resistivity vs temperature curve of GA / Pd bilayer (temperatures are computed from the liquid helium vapour pressure).

We shall demonstrate below the algorithm of Edwards *et al.* [ibid] to deconvolute the bolometer signal to obtain the incident phonon flux. The algorithm requires detailed measurements of the bolometer resistance-current calibration taken over a range of bath temperatures and such calibration data is displayed in Figure 3. The data was acquired under *LabView* computer control using a programmable *Hewlett-Packard* 34420A voltmeter and a *Keithley* 224 current source with a 4-wire technique (attached to the sample via two miniature *LakeShore* CC-C-25 coaxial cables). For each current magnitude, the current direction was reversed and an appropriate average taken to eliminate thermoelectric effects. The helium vapour pressure was controlled using an *LJ Engineering* 470-002 vacuum flow amplifier, a 484-002-1 electronic vacuum regulator, and a *Leybold Sogevac* UV25 vacuum pump. It was found that the temperature stability of this system was typically $<10^{-4}$ K over ~30 minute durations.

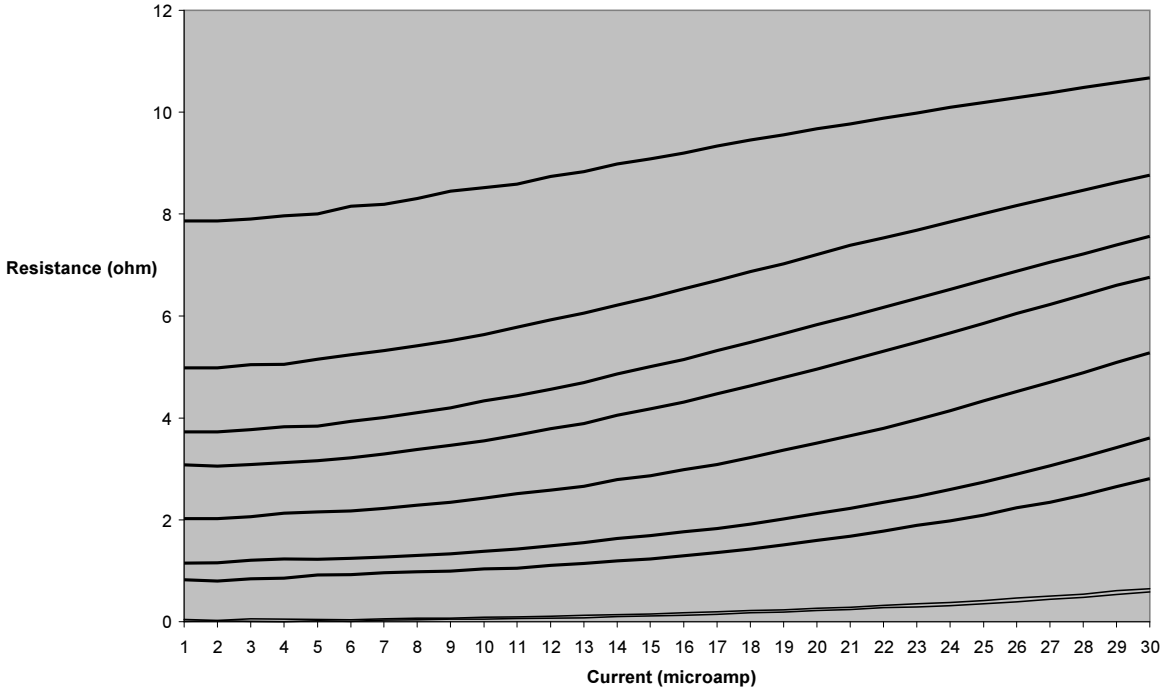

Figure 3. Bolometer resistance-current calibration traces for a discrete set of LHe bath temperatures. Top to bottom traces: LHe bath temperatures 1.835 K, 1.810 K, 1.798 K, 1.792 K, 1.783 K, 1.775 K, 1.772 K, 1.761 K, 1.760 K.

A bolometer can be characterized by the following quantities [Sanna *ibid*]

(i) The zero frequency responsivity $R(\omega=0)$ (V/W), defined by ($\omega = 2\pi f$)

$$R(\omega = 0) = i(dR/dT)/G_e \qquad (1)$$

where i is the bias current, dR/dT (Ω/K) (= α) is the temperature derivative of the electrical resistance, and

$$G_e = G - i^2\alpha \qquad (2)$$

is the effective thermal conductance. As described in detail by Danilchenko *et al*[20], the thermal conductance G (W/K) linking the superconductor to the substrate and helium bath, and α may both be experimentally obtained from the resistance-current calibration data in terms of a characteristic current

$$I_m = \sqrt{G/\alpha}\,. \qquad (3)$$

I_m is obtained from an appropriate fit to an R-I curve at the bias temperature of interest.

(ii) The effective time constant Λ (s) which characterizes the bolometer speed of response, is defined by

$$\Lambda = C/G_e \qquad (4)$$

where C (J/K) is the bolometer heat capacity. From a photoexcitation experiment with a fast laser pulse, one may, by measuring the decay time, deduce the effective heat capacity of the bolometer at the operating bias current and temperature. The frequency-dependent responsivity is given by

$$R(\omega) = R(0)/\sqrt{1+(\omega\Lambda)^2} \qquad (5)$$

(iii) The total noise power P_n which determines the minimum power detectable by the instrument. Measurements of the total noise power for our bolometers must await a future investigation.

The various parameters for our microbolometer are tabulated in Table 3 below. The responsivities have not been directly verified experimentally with a photoexcitation source of well-defined power. The effective time constants have been directly measured by photoexcitation with a pulsed mini-YAG laser with a 0.9-ns pulsewidth. In our experiments, the bolometer signals are first amplified with 2.8-GHz ac-coupled *Avtech* (26-dB 135A or 34-dB 135B) pulse amplifiers before acquisition with a *LeCroy WavePro950* 1-GHz digital oscilloscope. The effective risetime of the signal recovery electronics is approximately 300-ps.

Table 3. *Parameters of the superconducting granular aluminium/palladium microbolometer.*

Bias current i_0	10 μA	20 μA
Operating temperature θ_0	1.802 K	1.793 K
Bolometer resistance R_b	5 Ω	5 Ω
Characteristic current I_m (nominal value 25 μA used below)	25 ± 5 μA	same
Responsivity $R(i_0,\theta_0)$ (f=0)	1.8×10^4 V/W	1.3×10^5 V/W
Thermal conductance $G\|\theta_0$	9×10^{-8} W/K	same
$\partial R / \partial T \|i_0 \equiv \alpha$	1.3×10^2 Ω/K	1.6×10^2 Ω/K
Effective thermal conductance G_e	7.4×10^{-7} W/K	2.4×10^{-8} W/K
Effective time constant Λ	0.8 ns	12 ns
Heat capacity C	6×10^{-17} J/K	3×10^{-16} J/K

Figure 4 shows the response (solid curve) of a photoexcited bolometer, operating at a bias current of 10 μA and temperature of 1.802 K, to an unfocused and attenuated 0.75 ns 532 nm laser pulse. The effective time constant (20-80% falltime) is 0.8 ns. The bolometer signal was averaged over 4000 pulses. A rather severe undershoot is observed that we believe is due to excessive lead length (1-cm) of the microcoaxial cable that supplies the bias current. Each lead of the latter is wrapped 5 times around a toroidal magnet and terminated with magnetic beads. For comparison, the normalized response of a *Newport* 818-BB20 1.5-GHz silicon diode detector to the same photoexcitation, is shown as a dashed curve. The diode response was captured with a 2.8 GHz *SRS* boxcar integrator. The measured risetime of the diode response is approximately 300-ps.

Figure 5 shows (the upper curve) a 4000-shot average of an amplified photoexcited bolometer that is operating at 20 μA and 1.793 K. Once notices that the average decay is 12-ns and does not follow a single exponential. Rather, the initial recovery is somewhat steeper than the later slope. This effect has also been previously observed and explained by Edwards *et al* (ibid), i.e., for a larger ΔT excursion (~35-mK), the instantaneous bias current was less than i_0, so that the bolometer temperature was decaying towards a value actually less than the ambient temperature. The lower curve is the deconvoluted absorbed power as obtained by the algorithm of Edwards *et al* (ibid). We have implemented the algorithm in *LabView* and used the values of C and G as estimated in Table 3 as the only adjustable parameters. The temporal profile of the deconvoluted absorbed power matches rather well that of temporal profile of the photoexcitation pulse (displayed as the dash curve in Figure 3), i.e., both show a width of approximately 2 ns.

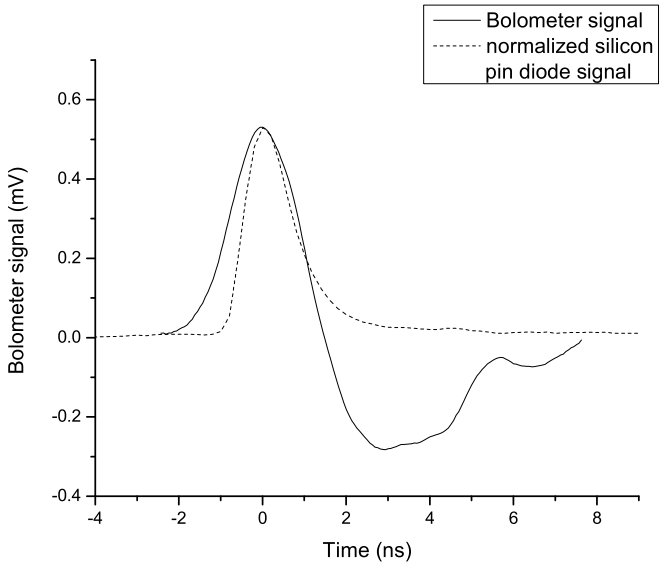

Figure 3 Averaged (4000 shots) bolometer signal (solid curve) biased at 10 μA and a normalized pin diode signal (dashed line) of mini-YAG. Bolometer signal displays a severe undershoot after the decay near 1 ns due to stray capacitance/inductance of the microcoax leads that supply the bias current.

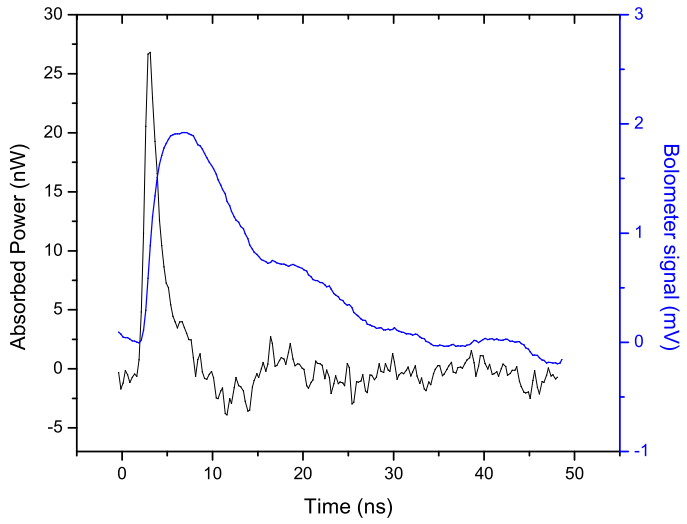

Figure 4. Averaged (4000 shots) bolometer signal (smoother upper trace) in mV, biased at 20 μA and the deconvoluted absorbed power (noisier lower trace) in nW. The noise is attributed to the calculation of the time derivative of the temperature excursion.

The estimated bolometer responsivity computed from the data displayed in Figure 5, taking into account the amplifier x20 gain, is approximately 3.5 x 10^3 V/W. The 3-dB cutoff in the frequency response of the responsivity R occurs at $f_{3dB} = 1/(2\pi\Lambda) = 13$ MHz. The bandwidth of the laser pulse is approximately 1 GHz and $R(f = 1GHz) = R(0)/\sqrt{1+(1GHz/13MHz)^2}$ = 1.7 x 10^3 V/W so that the two independent measurements of the bolometric high-frequency responsivity agree within an order of magnitude.

Finally, Figure 6 shows the microbolometer signal (upper curve) corresponding to the arrival of a [100] longitudinal acoustic phonon heat pulse that was optically excited by a pulsed mini-YAG laser [21] (0.75 ns pulse width, 532 nm wavelength, 0.5 μJ pulse energy) focused (50 μm diameter) directly opposite the bolometer on the rear of the substrate. The heat pulse was created in a niobium grating-coupler film, fabricated (using the above processing steps) on the front face of the 5 mm x 7 mm x 0.5 mm thick [100] Si:B (30-60 Ω-cm) die. The SC GA/Pd bilayer microbolometer is located on the rear sample face. The bolometer was biased at 20 μA. The bolometer trace shows an initial peak near 5 ns, due to scattered laser light directly illuminating the bolometer, and a second larger peak corresponding to the arrival of a ballistic longitudinal acoustic (LA) phonon pulse with a slowly-decaying diffusive tail. The LA phonon time-of-flight (60 ns) is in good agreement with the LA group velocity (8.5 x 10^6 mm/s) and the sample thickness (0.5 mm). The lower trace is the deconvoluted phonon flux that was computed using the bolometer thermal conductance G and heat capacity C as the only two free parameters. One notices that deconvolution accurately extracts the temporal profiles from the raw bolometer signal for both the scattered laser pulse and the LA phonon heat pulse, i.e., ~2-5 ns.

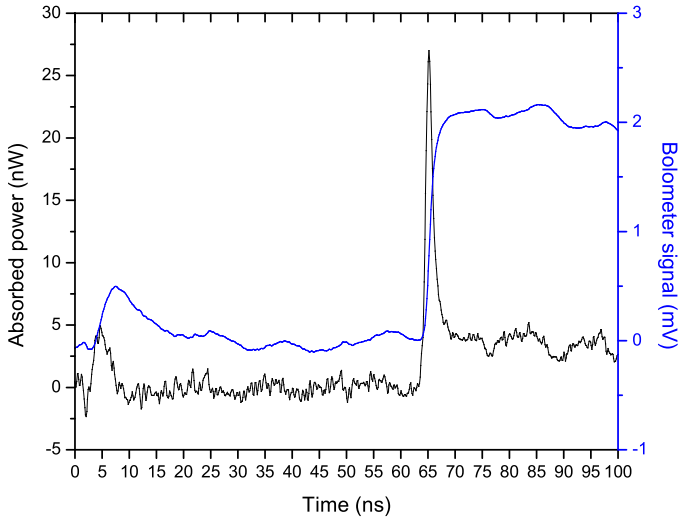

Figure 5. Averaged (4000 shots) bolometer signal (upper trace) corresponding to the arrival of an [100] LA heat pulse generated by the focused mini-YAG laser onto a Nb grating-coupler on the front of the [100] silicon substrate. Also shown is the deconvoluted phonon flux (lower trace). Deconvolution correctly yields the pulsewidths of the scattered laser light directly illuminating the bolometer, and the LA ballistic heat pulse. The slower decay is attributed to diffusive LA scattering. No evidence of TA phonons is seen.

We also note that there are alternatives to the popular SC GA bolometer that operate over a larger temperature range (1.2-3.5 K) and with better controllability of the normal state resistance and the SC transition temperature [Giltrow *ibid*]. We hope that the lithography recipe described herein may be useful in general however.

Acknowledgements. We acknowledge the support of the US Army Research Office: Program of *Theoretical Physics and Nonlinear Phenomena*, under contract numbers DAAD19-01-1-0466 and DAAHO4-96-1-0401. We appreciated the training and assistance provided by the faculty and staff at the University of Delaware ECE Nanofabrication Facility, including Brian Willis, Ranjani Sirdeshmukh, and Kjeld Krag-Jensen. Mashiur Rahman at Marshall University assisted with HF and piranha cleans. Finally, we acknowledge the encouragement of Werner Dietsche and Hanns-Ulrich Habermeier during discussions at the Max Planck Institute for Solid State Physics in Stuttgart, FRG.

References

[1] 15 April 2006 Proceedings of the 11th International Workshop on Low Temperature Detectors LTD-11, *Nuclear Instrum. Methods Physics Research A* **559** (2) 782-784

[2] Wigmore J K, Kozorezov A G, Hamid bin Rani, Giltrow M, Kraus H and Taele B M 2002 Scattering of THz phonons *Physica B* **316/317** 589

[3] K D Irwin, G C Hilton, D A Wollman, and John M Martinis 1998 Thermal-response time of superconducting transition-edge microcalorimeters *J. Appl. Phys.* **83** (8) 3978-3985.

[4] Rani H bin, Edwards S C, Wigmore J K and Collins R A 1988 Observation of heat pulses scattered from ion bombardment damage at sapphire surfaces *J. Phys. C: Solid State Phys.* **21** L701-707

[5] S C Edwards, Hamid bin Rani and J K Wigmore 1989 The use of superconducting bolometers for detecting nanosecond heat pulses, *J. Phys. E: Sci. Instrum* **22** 582-86

[6] J A Shields, M E Msall, M S Carroll, and J P Wolfe 1993 Propagation of optically generated acoustic phonons in Si, *Phys. Rev. B* **47** (19) 12510-12526

[7] G Sanna, M Nardi, and L Martinis 1990 Apparatus for the study of the IR multiple-photon resonances of polyatomic molecules via the optothermal technique. II. The superconducting bolometer, *Rev. Sci. Instrum.* **61** (5) 1379-1389

[8] H Kraus 1996 Superconductive bolometers and calorimeters, *Supercond. Sci. Technol.* **9** 827-842

[9] M Giltrow, M J Blylett, N S Lawson, A Hammiche, O J Griffiths, J K Wignmore and V Efimov 2003 The fabrication and characterization of polycrystalline CuSn bolometers, *Meas. Sci. Technol.* **14** N69-N71

[10] James P Wolfe 1998 *Imaging Phonons: Acoustic Wave Propagation in Solids* (New York, NY USA, Cambridge University Press)

[11] Daniel L Meier, John X Przybysz and Joonhee Kang 1991 Fabrication of an all-refractory circuit using lift-off with image-reversal lithography, *IEEE Trans. Magnetics* **27** (2) 3121-24; Product Data Sheet "AZ 5214 E Image Reversal Photoresist", AZ Electronic Materials, 70 Meister Avenue, Somerville, NJ 08876 USA

[12] 1 part H_2O_2 added to 7 parts H_2SO_4 (rapidly heats upon mixing)

[13] Headway Research Inc., 3713 Forest Lane, Garland, TX 75042 USA

[14] Catalog number AV125EORG, Whatman Inc., 9 Bridewell Place, Clifton, NJ 07014 USA

[15] SUSS MicroTec Inc., 228 SUSS Drive, Waterbury Center, VT 05677-0157 USA; Adtek Photomask 4950 Fisher Street Montreal, QC H4T 1J6 CANADA; Tanner Research, 2650 East Foothill Boulevard, Pasadena, CA 91107 USA

[16] Denton Vacuum Inc., 1259 North Church St., Moorestown, NJ 08057 USA

[17] Edwards model number LV10K, Kurt J Lesker Company, PO Box 10, 1925 Route 51, Clairton, PA 15025 USA

[18] R C Dynes and J P Garno 1980 Metal-insulator transition in granular aluminum, *Phys. Rev. Lett.* **46** (2), 137-40

[19] G Brammertz, A A Golubov, P Verhoeve, R den Hartog, A Peacock and H. Rogalla 2002 Critical temperature of superconducting bilayers: theory and experiment, *App. Phys. Lett.* **80** (16) 2955-57

[20] B Danilchenko, Cz Jaziukiewicz, T Paszkeiwicz, and S Wolski 2003 Response of Superconductor Bolometer to Phonon Fluxes, *Acta Physica Polonica A* **103** (4) 325-337

[21] Model *NanoGreen* NG-10320-010, JDS Uniphase, 1768 Automation Highway, San Jose, CA 95131 USA